



ARTICLE

<https://doi.org/10.1038/s42003-019-0351-4>

OPEN

The calcium channel subunit gamma-4 is regulated by MafA and necessary for pancreatic beta-cell specification

Cheng Luan¹, Yingying Ye¹, Tania Singh², Mohammad Barghouth¹, Lena Eliasson ¹, Isabella Artner ^{1,2}, Enming Zhang¹ & Erik Renström¹

Voltage-gated Ca^{2+} (Ca_v) channels trigger glucose-induced insulin secretion in pancreatic beta-cell and their dysfunction increases diabetes risk. These heteromeric complexes include the main subunit α_1 , and the accessory ones, including subunit gamma that remains unexplored. Here, we demonstrate that Ca_v gamma subunit 4 ($\text{Ca}_v\gamma_4$) is downregulated in islets from human donors with diabetes, diabetic Goto-Kakizaki (GK) rats, as well as under conditions of gluco-/lipotoxic stress. Reduction of $\text{Ca}_v\gamma_4$ expression results in decreased expression of L-type $\text{Ca}_v1.2$ and $\text{Ca}_v1.3$, thereby suppressing voltage-gated Ca^{2+} entry and glucose stimulated insulin exocytosis. The most important finding is that $\text{Ca}_v\gamma_4$ expression is controlled by the transcription factor responsible for beta-cell specification, MafA, as verified by chromatin immunoprecipitation and experiments in beta-cell specific MafA knockout mice (*MafA^{4 β cell}*). Taken together, these findings suggest that $\text{Ca}_v\gamma_4$ is necessary for maintaining a functional differentiated beta-cell phenotype. Treatment aiming at restoring $\text{Ca}_v\gamma_4$ may help to restore beta-cell function in diabetes.

¹Lund University Diabetes Center, Department of Clinical Sciences Malmö, Lund University, 202 13 Malmö, Sweden. ²Stem Cell Center, Department of Laboratory Medicine, Lund University, 221 85 Lund, Sweden. These authors contributed equally: Yingying Ye, Tania Singh, Mohammad Barghouth. Correspondence and requests for materials should be addressed to I.A. (email: isabella.artner@med.lu.se) or to E.Z. (email: enming.zhang@med.lu.se) or to E.R. (email: erik.renstrom@med.lu.se)

Pancreatic beta-cell failure is central in diabetes mellitus¹. Deteriorated insulin secretion arises from a damaged secretory machinery or reduced beta-cell mass, collectively referred to as functional beta-cell mass. Insulin secretion is triggered by Ca^{2+} entry via voltage-gated Ca^{2+} (Ca_V) channels, activation of the Ca^{2+} sensor synaptotagmin, and exocytosis of docked insulin granules². Ca_V channels are heteromeric complexes including the pore-forming $\alpha 1$ subunits and accessory beta, $\alpha 2\delta$ and gamma subunits³. The best-studied are $\text{Ca}_V \alpha 1$ that have specific roles in phasic insulin secretion^{3,4}. The accessory Ca_V beta and $\alpha 2\delta$ determine ion channel trafficking and membrane targeting^{5,6}. However, the least studied are the eight Ca_V gamma ($\text{Ca}_V\gamma$) variants, and reports are contradictory⁷. For example, gamma1 inhibits L-type $\text{Ca}_V 1.1$ channels in skeletal muscle, but physically associates with cardiac L-type $\text{Ca}_V 1.2$ (refs. 8,9). Notably, $\text{Ca}_V\gamma$ subunits were shown to bind with voltage-sensing domain IV (VSD_{IV}) in $\alpha 1$ subunits¹⁰. The functions of the voltage-gated Ca^{2+} channel subunit gamma4 ($\text{Ca}_V\gamma 4$) are largely unknown, but it is widely detected in many tissues¹¹.

Furthermore, Ca^{2+} signals influence functional beta-cell mass and development of diabetes. For instance, common genetic variations in the genes encoding L-type $\text{Ca}_V 1.3$ and R-type $\text{Ca}_V 2.3$ affect beta-cell functionality or risk of type-2 diabetes (T2D)^{12,13}. Beta-cell mass reduction leading to diabetes may be induced by apoptosis as a consequence of, e.g., autoimmunity or endoplasmic reticulum (ER) stress¹⁴. However, recent evidence suggests that functional beta-cell mass reduction may be due to beta-cell dedifferentiation rather than cell death¹⁵. Previous reports point to Ca^{2+} signaling by Ca_V channels being a regulator of beta-cell mass through control of differentiation. For example, ablation of the $\alpha 1$ subunit $\text{Ca}_V 1.3$ in mice decreases both the number and size of islets compared to wild type, without affecting beta-cell death¹⁶. In $\text{Ca}_V 2.3$ knockout mice, islet cell differentiation also seemed imperfect, suggestive of a role in beta-cell differentiation⁴. Additionally, pharmacological inhibition of Ca_V channels in neonatal rat pancreata by diltiazem markedly decreases beta-cell proliferation¹⁷. Concerning the $\text{Ca}_V\gamma$, gamma4 is the only one shown to be involved in differentiation, e.g., in the fetal brain and differentiating myoblasts¹⁸. Collectively, these reports show that Ca_V channels influence the signaling pathway of differentiation, but the underlying molecular mechanisms remain unknown.

Several transcription factors control pancreatic cell lineage differentiation and specification, e.g. Pdx1, necessary for pancreas development, Nkx6.1, and MafA that determine the final maturation into beta cells^{19,20}. Genes targeted by MafA include Ca^{2+} signaling molecules, such as $\text{Ca}^{2+}/\text{CamkII}$ ^{20,21}. In line with the idea that beta-cell loss in T2D occurs by dedifferentiation rather than apoptosis, Pdx1, MafA, and Nkx6.1 are downregulated under such conditions^{15,22,23}.

In this study, we have employed systems biology approaches to address the roles Ca_V channels play in beta-cell differentiation, in combination with physiological validation that identifies the $\text{Ca}_V\gamma 4$ as a downstream target of MafA. $\text{Ca}_V\gamma 4$ controls expression of other Ca_V subunits and affects Ca_V channel electrophysiology. Downregulation of $\text{Ca}_V\gamma 4$ occurs in islets from patients with T2D and from diabetic animal models, which suppresses insulin secretion. In conclusion, our results demonstrate that $\text{Ca}_V\gamma 4$ affects insulin exocytosis, but plays an even more important role in maintaining beta-cell differentiation and islet health.

Results

$\text{Ca}_V\gamma 4$ expression is reduced by gluco-/lipotoxic treatment. Analysis of human pancreatic islets mRNA microarray database²⁴

displayed that among all $\text{Ca}_V\gamma$ subunits $\text{Ca}_V\gamma 4$ (*CACNG4*) was notably downregulated in individuals with higher glycated hemoglobin (HbA1c) values (Supplementary Fig. 1a). Altered $\text{Ca}_V\gamma 4$ expression was confirmed in human islets by qPCR, but not for $\text{Ca}_V\gamma 5$ nor $\text{Ca}_V\gamma 8$ ($p = 0.045$, 0.294 , and 0.395 , respectively; Fig. 1a). See also Supplementary Table 1 for the characteristics of human islet donors used experimentally in current study). Confocal immunocytochemistry revealed a marked loss of $\text{Ca}_V\gamma 4$ expression in beta cells from T2D human donors ($p = 0.029$; Fig. 1b, c). We then investigated several hyperglycemic or diabetic animal models. Interestingly, reduction of $\text{Ca}_V\gamma 4$ expression was found in islets from Goto-Kakizaki (GK) rats and *db/db* mice ($p = 0.036$ and 0.006 , respectively; Fig. 1d, e), but not in insulin mutant Akita mice (Fig. 1f). To establish these in vivo findings, we next determined $\text{Ca}_V\gamma 4$ expression under gluco-/lipotoxic conditions in vitro. Seventy-two hours culture in 20 mM glucose or 48 h culture with 1 mM palmitate both decreased $\text{Ca}_V\gamma 4$ protein expression in healthy Wistar rat islets ($p = 0.009$ and 0.011 , respectively; Fig. 1g, h). Accordingly, $\text{Ca}_V\gamma 4$ protein expression in human islets was also reduced after incubation in 20 mM glucose for 48 h (Supplementary Fig. 1b), but not for 72 h (Supplementary Fig. 7l), implying a compensatory mechanism for maintaining stable $\text{Ca}_V\gamma 4$ expression in human healthy beta cells under conditions of glucotoxicity. A similar reduction of $\text{Ca}_V\gamma 4$ was found in rat insulinoma INS-1 832/13 cells (Supplementary Fig. 1c, d). Taken together, these results suggest that $\text{Ca}_V\gamma 4$ is part of the response to glucotoxicity in pancreatic beta cells.

$\text{Ca}_V\gamma 4$ is required for glucose-stimulated insulin secretion. We next examined if changes in $\text{Ca}_V\gamma 4$ expression affect beta-cell function. First, glucose-stimulated insulin secretion (GSIS) was markedly inhibited in $\text{Ca}_V\gamma 4$ -silenced Wistar rat islets and non-diabetic human islets ($p = 0.006$ and 0.044 , respectively; Fig. 2a, c), and also in INS-1 cells (Supplementary Fig. 2b). Given the reduced $\text{Ca}_V\gamma 4$ expression under hyperglycemic conditions (Fig. 1), we next overexpressed $\text{Ca}_V\gamma 4$ to study effects of insulin secretion. This enhanced GSIS in Wistar rat islets (Supplementary Fig. 2a), but more importantly in both diabetic GK rat islets ($p = 0.028$; Fig. 2b) and in T2D human islets (Fig. 2d).

To explore further the impact of $\text{Ca}_V\gamma 4$ on beta-cell function, we performed capacitance recordings of single-cell exocytosis. In Wistar rat islets, a dramatic reduction of beta-cell exocytosis was detected when silencing $\text{Ca}_V\gamma 4$ as compared to control cells (389 ± 35 fF vs. 997 ± 206 fF, $p = 0.009$; Fig. 2e, f). A detailed analysis of the readily releasable insulin granules (phase 1) and the sustained phase 2 revealed a decline in both (153 ± 13 fF vs. 453 ± 109 fF, $p = 0.013$ and 236 ± 29 fF vs. 544 ± 126 fF, $p = 0.028$, respectively; Fig. 2f). As expected, $\text{Ca}_V\gamma 4$ overexpression enhanced overall exocytosis in GK rat beta cells (318 ± 50 fF vs. 190 ± 33 fF, $p = 0.042$; Fig. 2g, h). Successful silencing (by siRNA) or overexpression (by lentivirus) are verified by both qPCR and western blotting in human islets and cell lines (Supplementary Fig. 2c–g).

$\text{Ca}_V\gamma 4$ regulates Ca^{2+} influx via L-type Ca_V channels. The $\text{Ca}_V\gamma 4$ -related effects on insulin secretion (Fig. 2a–d, Supplementary Fig. 2a, b) and insulin granule exocytosis (Fig. 2e–h) seen so far might result from enhanced Ca^{2+} influx². Patch clamp offers a direct mode of detection, but it may also be observed in intracellular Ca^{2+} imaging. Therefore, we measured Ca^{2+} currents by patch clamp first, and the representative traces from both condition recordings are shown in Fig. 3a, b, left. Overexpressing $\text{Ca}_V\gamma 4$ in non-diabetic human beta cells increased whole-cell Ca^{2+} currents compared to control (-6.17 ± 0.52 pC vs. -4.71 ± 0.46 pC, $p = 0.048$; Fig. 3a, right). More strikingly, impaired

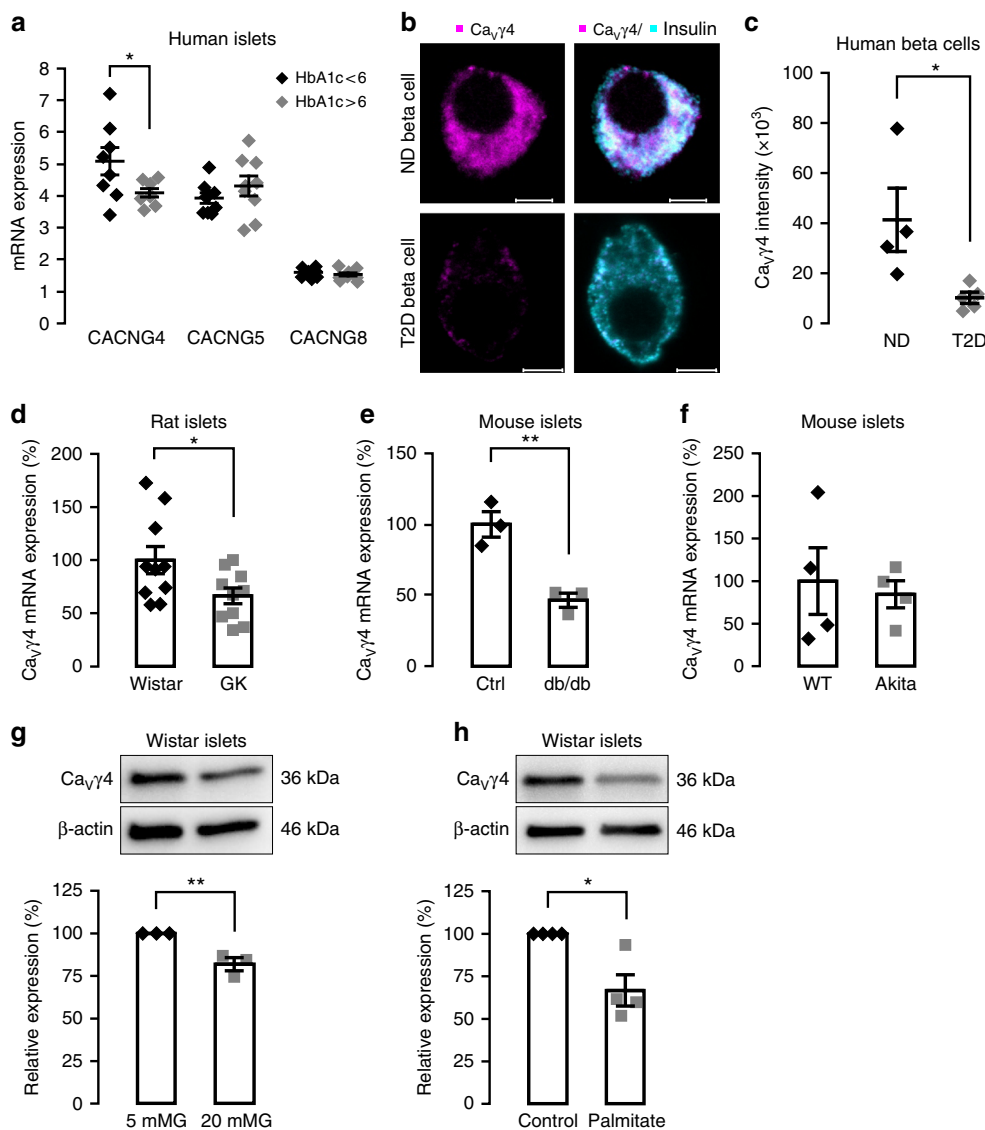


Fig. 1 Decreased $Ca_v\gamma 4$ expression in beta cells in diabetes and in response to glucotoxicity. **a** $Ca_v\gamma 4$ (CACNG4), $Ca_v\gamma 5$ (CACNG5), and $Ca_v\gamma 8$ (CACNG8) mRNA expression in human islets from donors with HbA1c <6 and >6. $n = 8$ or 9 donors with age and gender matched, $*p = 0.045$ (CACNG4), $p = 0.294$ (CACNG5), $p = 0.395$ (CACNG8). **b** Representative immunofluorescence images of $Ca_v\gamma 4$ expression in human islet beta cells from non-diabetic (ND) and T2D donor. Scale: 5 μm . $Ca_v\gamma 4$ in magenta and insulin in cyan (7–11 beta cells were analyzed per each T2D donor, and 5–7 beta cells for each ND donor). **c** Calculation of fluorescent intensity for $Ca_v\gamma 4$. $n = 4$ ND and 5 T2D donors (5–11 beta cells were analyzed per donor), $*p = 0.029$. **d** Decreased $Ca_v\gamma 4$ mRNA expression in Goto-Kakizaki (GK) rat islets. $n = 10$ rats each, $*p = 0.036$. **e** As in **d** but in *db/db* mouse islets. $n = 3$ mice each, $**p = 0.006$. **f** $Ca_v\gamma 4$ mRNA expression in wild type and Akita mouse islets. $n = 4$ mice each, $p = 0.727$. **g** Decreased $Ca_v\gamma 4$ protein expression in Wistar rat islets cultured at 5 or 20 mM glucose (72 h). $n = 3$, $**p = 0.009$. **h** As in **g** but cultured with 1 mM palmitate (48 h). $n = 4$, $*p = 0.011$. Data are presented as mean \pm SEM and were analyzed with two-tailed unpaired Student's *t*-test. See also Supplementary Table 1 for the details of the human donors utilized for experiments in this study. WT wild type, Ctrl control

Ca^{2+} influx in T2D human beta cells was rescued by correcting the reduced $Ca_v\gamma 4$ expression levels (-4.82 ± 0.45 pC vs. -2.95 ± 0.26 pC at 0 mV, $p = 0.004$; Fig. 3b, right). Validation in rodent islets showed that silencing $Ca_v\gamma 4$ decreased Ca^{2+} influx in Wistar rat beta cells (Fig. 3c), whereas augmented Ca^{2+} influx was recorded in $Ca_v\gamma 4$ -overexpressing GK and Wistar rat beta cells (Fig. 3d, e).

Next, measurements of intracellular Ca^{2+} concentration ($[Ca^{2+}]_i$) were done in INS-1 cells. Upon 70 mM KCl stimulation, both the initial $[Ca^{2+}]_i$ peak and the integrated Ca^{2+} load were markedly lower in $Ca_v\gamma 4$ -silenced cells as compared to control cells ($12.6 \pm 0.6 F_i/F_0$ vs. $19.5 \pm 1.1 F_i/F_0$, $p < 0.001$ and 888.5 ± 50 AUC (area under the curve) vs. 1084.5 ± 48 AUC, $p = 0.006$,

respectively; Fig. 3f–h), in agreement with above electrophysiology results. By contrast, $Ca_v\gamma 5$ silencing induced the increase of both $[Ca^{2+}]_i$ peak and Ca^{2+} load (Fig. 3f–h), however, no changes in $Ca_v\gamma 8$ -silencing cells (Supplementary Fig. 3a, b). Additionally, 16.7 mM glucose, a more physiological stimulus, exerted similar effect on $Ca_v\gamma 4$ -abolished cells, but not on $Ca_v\gamma 5$ -silenced cells (Fig. 3i–k). Ca^{2+} currents recorded in $Ca_v\gamma 5$ - or $Ca_v\gamma 8$ -silenced INS-1 cells showed no or increased effects, respectively (Supplementary Fig. 3c, d).

Subsequently, we studied the specific involvement of the different pore-forming $\alpha 1$ subunits in $Ca_v\gamma 4$ mediated Ca^{2+} influx. Intriguingly, when L-type Ca^{2+} currents were pharmacologically inhibited by isradipine (2 μM), an L-type Ca^{2+} channel

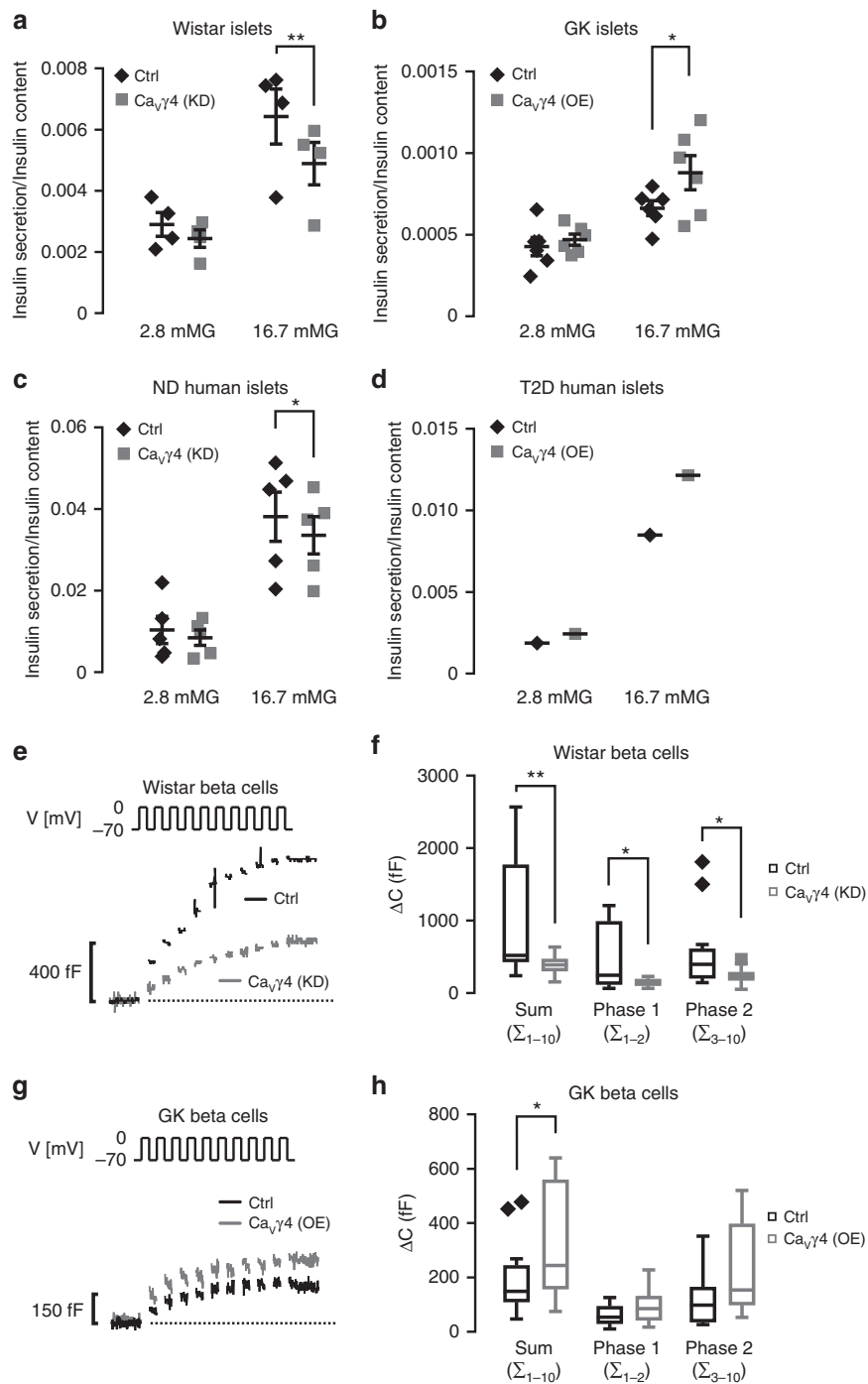
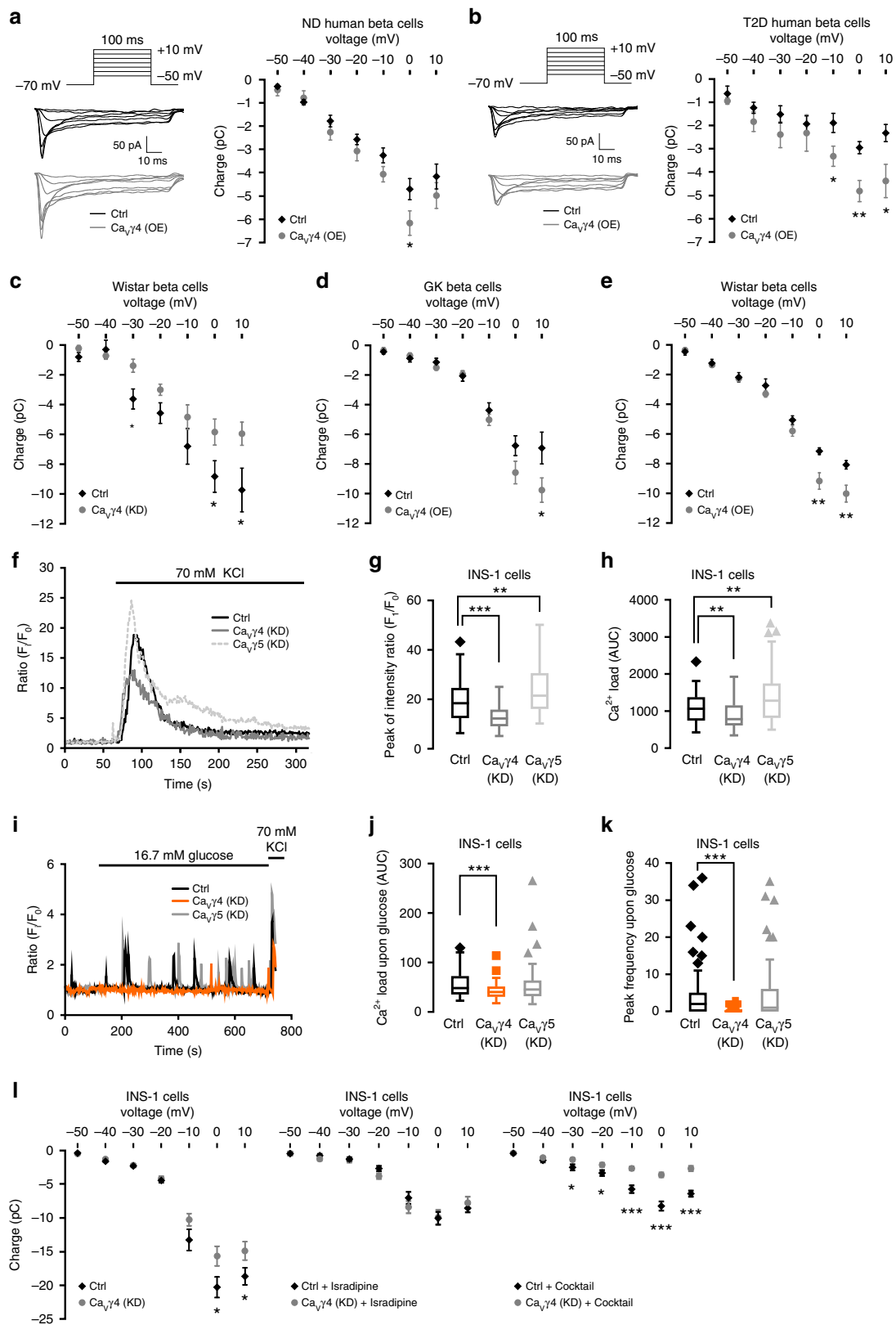


Fig. 2 Impact of Ca_vγ4 on beta-cell function. **a** Glucose-stimulated insulin secretion (GSIS) in Ca_vγ4-silenced Wistar rat islets. $n = 4$, $**p = 0.006$. **b** As in **a** but in Ca_vγ4-overexpressed GK rat islets. $n = 6$, $*p = 0.028$. **c** As in **a** but in Ca_vγ4-silenced non-diabetic (ND) human islets. $n = 5$ donors, $*p = 0.044$. **d** As in **a** but in Ca_vγ4-overexpressed T2D human islets. $n = 1$ donor ($p = 0.008$ in 16.7 mMG group by six technical repeats). **e** Reduced depolarization-evoked (V) exocytosis in Ca_vγ4-silenced Wistar rat beta cells measured as an increase in membrane capacitance (ΔC). **f** A summary of data in **e** presented as ΔC evoked by all 10 pulses of the train (Sum), the two first pulses (Phase 1) or the latter eight pulses (Phase 2). $n = 15$ control and 14 Ca_vγ4-silencing cells, $**p = 0.009$ (Sum), $*p = 0.013$ (Phase 1) and $*p = 0.028$ (Phase 2). **g** As in **e** but rescued exocytosis in Ca_vγ4-overexpressed GK rat beta cells. **h** Summary of data in **g**. $n = 15$ control and 16 Ca_vγ4-overexpressing cells, $*p = 0.042$ (Sum), $p = 0.07$ (Phase 1), and $p = 0.058$ (Phase 2). Data are presented as Mean \pm SEM and were analyzed with two-tailed paired (**a-c**) or unpaired (**f, h**) Student's *t*-test. OE overexpression, KD knockdown

blocker, silencing of Ca_vγ4 failed to further suppress Ca²⁺ influx in INS-1 cells (Fig. 3| left, middle). Importantly, when using a cocktail of non-L-type channel blockers (100 nM ω-agatoxin IVA, 50 nM ω-conotoxin GVIA, and 100 nM SNX-482), silencing of Ca_vγ4 retained its suppressive action on Ca²⁺ influx (Fig. 3|, right).

Ca_vγ4 associates with L-type Ca_v channel expression. Next, we explored how Ca_vγ4 associates with the different L-type Ca_v channels. First, human islets microarray data showed a strong positive correlation between Ca_vγ4 and L-type Ca_v subunits known to be involved in human insulin secretion, Ca_v1.2 (*CACNA1C*), and Ca_v1.3 (*CACNA1D*), whereas it displayed no



correlation between $Ca_v\gamma4$ and $Ca_v1.1$ (*CACNA1S*) or $Ca_v1.4$ (*CACNA1F*) (Fig. 4a). Interestingly, silencing $Ca_v\gamma4$ resulted in downregulation of both $Ca_v1.2$ and $Ca_v1.3$ gene expression in non-diabetic human islets ($p = 0.032$ and 0.011 , respectively; Fig. 4b). Meanwhile, the $Ca_v1.2$ and $Ca_v1.3$ mRNA levels were elevated by overexpressing $Ca_v\gamma4$ in non-diabetic human islets

($p = 0.005$ and 0.039 , respectively; Fig. 4c), as well as in T2D human islets (Supplementary Fig. 4a). Similarly, depleting $Ca_v\gamma4$ reduced protein levels of $Ca_v1.2$ and $Ca_v1.3$ in INS-1 cells, and also the levels of Ca_v alpha2delta ($Ca_v\alpha2\delta1$), but increased the protein expression of beta subunits ($Ca_v\beta1$) ($p < 0.001$ for all; Fig. 4d); findings correlating with changes in mRNA

Fig. 3 Boost of Ca^{2+} influx in $\text{Ca}_V\gamma 4$ -overexpressed beta cells. **a** Ca^{2+} currents records in $\text{Ca}_V\gamma 4$ -overexpressed non-diabetic (ND) human beta cells. $n = 12$ control and 13 $\text{Ca}_V\gamma 4$ -overexpressing cells (4 donors), $*p = 0.048$. **b** As in **a** but in T2D human beta cells. $n = 7$ control and 8 overexpressing cells (1 T2D donor), $*p = 0.032$ (-10 mV), $**0.004$ (0 mV), $*0.028$ (10 mV). **c** As in **a** but in $\text{Ca}_V\gamma 4$ -silenced Wistar rat beta cells. $n = 15$ control and 14 silencing cells, $*p = 0.040$ (0 mV), $*0.034$ (10 mV). **d** As in **a** but in $\text{Ca}_V\gamma 4$ -overexpressed GK rat beta cells. $n = 15$ control and 14 overexpressing cells, $*p = 0.047$. **e** As in **a** but in $\text{Ca}_V\gamma 4$ -overexpressed Wistar rat beta cells. $n = 16$ cells each, $**p = 0.003$ (0 mV), $**0.006$ (10 mV). **f** Ca^{2+} imaging in control, $\text{Ca}_V\gamma 4$, or $\text{Ca}_V\gamma 5$ silenced INS-1 cells. **g** Comparisons of $[\text{Ca}^{2+}]_i$ peak intensity (F_i/F_0) in **f**, $***p < 0.001$ ($\text{Ca}_V\gamma 4$), $**p = 0.001$ ($\text{Ca}_V\gamma 5$). **h** Integrated Ca^{2+} load (AUC) in **f**, 0–180 s after stimulation. $**p = 0.006$ ($\text{Ca}_V\gamma 4$), $**p = 0.002$ ($\text{Ca}_V\gamma 5$). $n = 62$ control, 53 $\text{Ca}_V\gamma 4$ - and 61 $\text{Ca}_V\gamma 5$ -silencing cells from three independent experiments for both **g** and **h**. **i** As in **f** but by stimulation of glucose. **j** As in **h** but 0–600 s after glucose stimulation. $***p < 0.001$ ($\text{Ca}_V\gamma 4$) (n.s., $\text{Ca}_V\gamma 5$). **k** Frequency of $[\text{Ca}^{2+}]_i$ peaks (counted as $F_i/F_0 > 1.5$) during stimulation. $***p < 0.001$ ($\text{Ca}_V\gamma 4$) (n.s., $\text{Ca}_V\gamma 5$). $n = 60$ control, 62 $\text{Ca}_V\gamma 4$ - and 61 $\text{Ca}_V\gamma 5$ -silencing cells for both **j** and **k**. **l** Left: As in **a** but in $\text{Ca}_V\gamma 4$ -silenced INS-1 cells. $n = 32$ control and 37 silencing cells, $*p = 0.031$ (0 mV), $*0.049$ (10 mV). Middle: in the presence of $2 \mu\text{M}$ isradipine. $n = 12$ control and 14 silencing cells. Right: or non-L-type channel blocker cocktail (100 nM ω -agatoxin IVA, 50 nM ω -conotoxin GVIA, and 100 nM SNX-482). $n = 15$ control and 21 silencing cells, $***p < 0.001$. Data are presented as mean \pm SEM and were analyzed with two-tailed unpaired Student's *t*-test; the significance in **g**, **h**, **j**, **k** was corrected by the Holm-Bonferroni method. OE overexpression, KD knockdown

(Supplementary Fig. 4b). Additionally, $\text{Ca}_V1.2$ expression was clearly reduced in glucose- or palmitate-challenged Wistar rat islets ($p = 0.003$ both; Fig. 4e, f) and INS-1 cells (Supplementary Fig. 4c). Intriguingly, 24-h treatment with 20 mM glucose reduced the direct spatial interaction between $\text{Ca}_V\gamma 4$ and $\text{Ca}_V1.3$ detected by proximity ligation assay ($p < 0.001$; Fig. 4g, h). This dissociation, under hyperglycemic condition, could reflect an altered affinity between the subunits or simply be due to the lower expression of $\text{Ca}_V\gamma 4$ (see Fig. 1). For $\text{Ca}_V1.2$, we failed to detect interaction, the significance of which remains uncertain.

MafA mediates $\text{Ca}_V\gamma 4$ expression in beta cells. Given the surprisingly important role of $\text{Ca}_V\gamma 4$ in beta cells, the factors that regulate $\text{Ca}_V\gamma 4$ expression are of special interest. Furthermore, pathophysiological alterations observed above when depleting $\text{Ca}_V\gamma 4$ are reminiscent of a dedifferentiated diabetic beta-cell phenotype. We therefore explored genes involved in pancreas or beta-cell development, for co-regulation with $\text{Ca}_V\gamma 4$ in human islets microarray (Fig. 5a). These data revealed a strong positive correlation between $\text{Ca}_V\gamma 4$ and the important beta-cell differentiation transcription factors *NEUROD1*, *MAFA*, *ISL1*, and *PDX1* (Supplementary Fig. 5a). To determine the causality of this correlation, *Pdx1*, *NeuroD1*, *MafA*, *Isl1*, and *Tcf7l2* were silenced in INS-1 cells, respectively (successful silencing has been proved previously²⁵), with *MafA* silencing having the largest effect on $\text{Ca}_V\gamma 4$ mRNA expression ($***p < 0.001$; Fig. 5b). Also $\text{Ca}_V\gamma 4$ protein levels were profoundly reduced after *MafA* silencing ($***p < 0.001$; Fig. 5c). Given that *MafA* is predominantly expressed in adult rodent beta cells as a selective beta-cell marker²⁶, and is found to be capable of reprogramming acinar cells to beta-like cells²⁰, moreover, *Pdx1*, *NeuroD1*, and *Isl1* are also expressed in other types of endocrine cells in islets^{27,28}. Against this backdrop, we further explored the effects of *MafA* on $\text{Ca}_V\gamma 4$. In beta-cell-specific *MafA* knockout mice (*MafA* ^{Δ beta}), $\text{Ca}_V\gamma 4$ protein levels were strongly reduced in vivo ($p = 0.001$; Fig. 5d). Confirmation in vitro showed that $\text{Ca}_V\gamma 4$ expression was notably decreased in *MAFA*/*MAFB* double-silenced human islets ($p = 0.005$; Fig. 5e). *MAFA* ablation alone failed to induce an alteration on $\text{Ca}_V\gamma 4$ expression (Supplementary Fig. 5b). This we attribute to the fact that human beta cells express both *MAFA* and *MAFB* while only *MafB* is detected in adult mouse alpha cells²⁹, which suggests a possible compensatory effect of *MAFB* in human beta cells. Furthermore, chromatin immunoprecipitation analysis disclosed two binding sites of *MafA* to $\text{Ca}_V\gamma 4$ promoter region ($**p < 0.01$; Fig. 5f), indicating that $\text{Ca}_V\gamma 4$ is directly regulated by *MafA*.

Downregulation of $\text{Ca}_V\gamma 4$ results in beta-cell dedifferentiation rather than other dysfunctions since the phenotype of $\text{Ca}_V\gamma 4$ -silenced beta cell as detailed above remains unaltered. Recently, a new beta-cell dedifferentiation marker aldehyde dehydrogenase1a3 (*Aldh1a3*) was found to be highly enriched in

dedifferentiated islets³⁰ and suggested marker of dedifferentiated beta cells in human type-2 diabetic islets²². Here, *ALDH1A3* gene expression was decreased in $\text{Ca}_V\gamma 4$ -overexpressed non-diabetic human islets ($p = 0.004$; Fig. 5g), whereas protein levels were markedly upregulated in $\text{Ca}_V\gamma 4$ -silenced INS-1 cells ($p = 0.008$, Fig. 5h). The results are perfectly consistent with data on co-expression of *ALDH1A3* with *CACNG4* by human islets microarray data (Supplementary Fig. 5c). Additionally, silencing $\text{Ca}_V\gamma 4$ failed to induce any alterations in cleaved Caspase-3 and P21 expression, cell viability (MTT) or apoptosis (7-AAD staining) (see Supplementary Fig. 5d–f), indicating beta-cell health is not influenced by $\text{Ca}_V\gamma 4$ expression.

Reduced Ca^{2+} currents in *MafA* ^{Δ beta} beta cells. We next tested the hypothesis as suggested above to the effect that *MafA* controls $\text{Ca}_V\gamma 4$ expression, which in turn has consequences for L-type Ca_V channels specific Ca^{2+} influx and function of beta cells. In support of this, Ca^{2+} currents were reduced in *MafA* ^{Δ beta} beta cells. Interestingly, and in accord with the hypothesis, the L-type Ca^{2+} channel blocker isradipine ($2 \mu\text{M}$) failed to affect Ca^{2+} influx (Fig. 6a). Conversely, the L-type Ca^{2+} channel agonist Bay K8644 (300 nM) potentiated Ca^{2+} influx in wild-type mouse beta cells, while being ineffective in *MafA*-depleted beta cells (Fig. 6b). Further support came from the observation that overexpressing $\text{Ca}_V\gamma 4$ in *MafA* ^{Δ beta} islets resulted in elevated beta-cell Ca^{2+} influx (Fig. 6c). In addition, the role of *MafA* in Ca^{2+} signaling was confirmed in INS-1 cells (Fig. 6d). As expected, reintroducing $\text{Ca}_V\gamma 4$ in *MafA* ^{Δ beta} islets raised both $\text{Ca}_V1.2$ and $\text{Ca}_V1.3$ mRNA expression ($p = 0.009$ and 0.005 , respectively; Fig. 6e), as well as in *MAFA* silenced human EndoC cells (Supplementary Fig. 6). Similar to data in Fig. 6a, b, Ca^{2+} imaging in *MafA* ^{Δ beta} and wild-type mouse beta cells exposed to Bay K8644 (300 nM) or isradipine ($2 \mu\text{M}$) (Fig. 6f, g) strongly substantiated the idea that L-type Ca^{2+} channels are downstream target of *MafA*, with impacting on Ca^{2+} influx in beta cells. Furthermore, we recorded an almost 50% rescue of exocytosis (particularly the readily releasable pool), in $\text{Ca}_V\gamma 4$ -overexpressing *MafA* ^{Δ beta} beta cells, restoring exocytosis at levels similar to that in wild-type beta cells (Fig. 6h). Finally, reduced GSIS was observed after silencing *MafA* in INS-1 cells (Fig. 6i).

These results suggest that *MafA* controls Ca^{2+} influx via an effect involving $\text{Ca}_V\gamma 4$ and L-type Ca_V channels, which eventually initiate insulin release. However, this pathway is affected at multiple sites by glucotoxicity and in diabetic conditions leading to a dedifferentiated and diabetes-prone phenotype (Fig. 7).

Discussion

$\text{Ca}_V\gamma$ subunits were first isolated in guinea pig skeletal muscle in the form of a complex with L-type Ca^{2+} channels and $\text{Ca}_V\gamma 1$ subunits³¹. $\text{Ca}_V\gamma 2$, $\text{Ca}_V\gamma 3$, $\text{Ca}_V\gamma 4$, and $\text{Ca}_V\gamma 8$ subunits

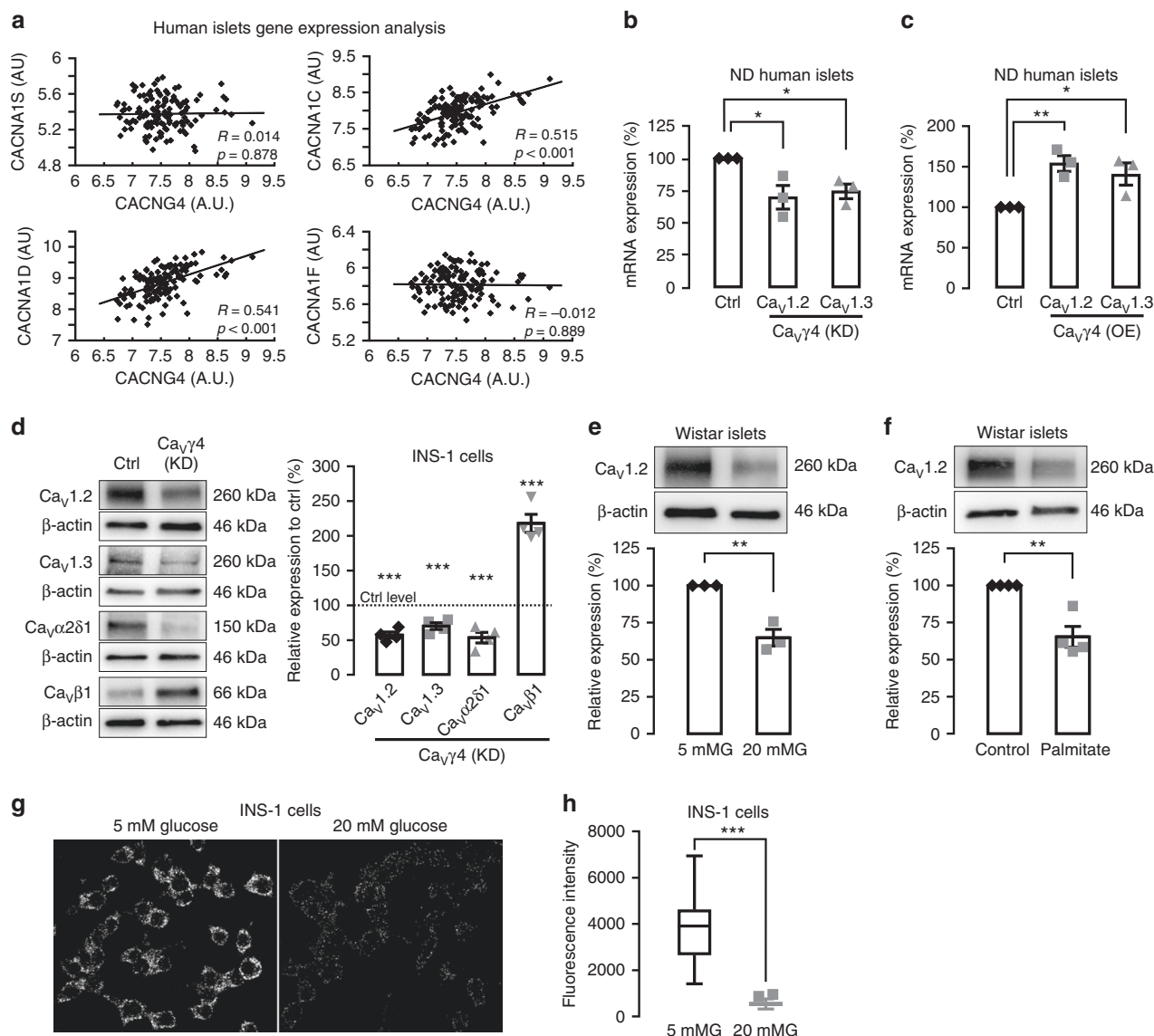
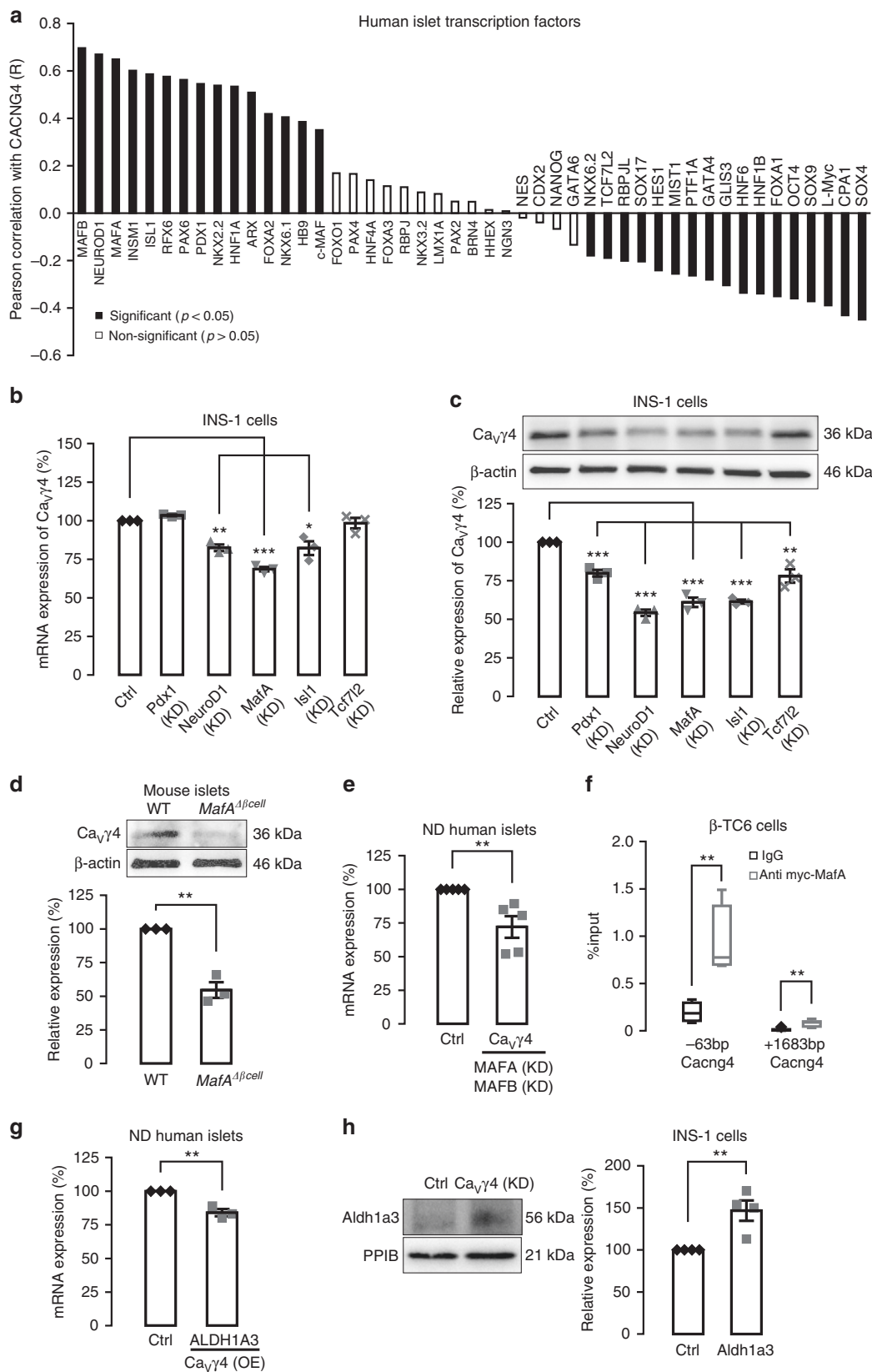


Fig. 4 Downregulation of L-type Ca_v channels in $Ca_v\gamma 4$ -silenced beta cells. **a** Correlation of mRNA expression (Microarray) between $Ca_v\gamma 4$ ($CACNG4$) and L-type Ca_v channels in human islets. $n = 128$ donors. Pearson correlation coefficient (R) was tested (t -test) and labeled alongside with p values. **b** $Ca_v1.2$ ($CACNA1C$) and $Ca_v1.3$ ($CACNA1D$) mRNA expression (qPCR) in $Ca_v\gamma 4$ -silenced human islets. $n = 3$ donors, $*p = 0.032$ ($Ca_v1.2$), $*p = 0.011$ ($Ca_v1.3$). **c** As in **b** but in $Ca_v\gamma 4$ -overexpressed human islets. $n = 3$ donors, $**p = 0.005$ ($Ca_v1.2$), $*p = 0.039$ ($Ca_v1.3$). **d** Ca_v channel immunoblotting and means of expression in $Ca_v\gamma 4$ -silenced INS-1 cells. $n = 4$, $***p < 0.001$. **e** Decreased $Ca_v1.2$ expression in Wistar islets cultured at 5 or 20 mM glucose (72 h). $n = 3$, $**p = 0.003$. **f** As in **e** but cultured with 1 mM palmitate (48 h). $n = 4$, $**p = 0.003$. **g** Interaction between $Ca_v\gamma 4$ and $Ca_v1.3$ in INS-1 cells treated with 5 or 20 mM glucose (24 h). Visualization by proximity ligation assay as fluorescent spots. **h** Calculation of fluorescent intensity. $n = 25$ cells each, $***p < 0.001$. Data are presented as mean \pm SEM and were analyzed with two-tailed unpaired Student's t -test; and the significance in **b**, **c** was corrected by the Holm-Bonferroni method. OE overexpression, KD knockdown

have later been shown to associate with AMPA receptors in neurons^{32,33}, but $Ca_v\gamma 4$ and $Ca_v\gamma 8$ are demonstrated to physically interact with the cardiac L-type Ca^{2+} channel $Ca_v1.2$ (ref. 9). The rationale for focusing on $Ca_v\gamma 4$ stems from it being the only differentially expressed $Ca_v\gamma$ subunit in human diabetic islets (Fig. 1a). Furthermore, $Ca_v\gamma 4$ is also downregulated in hyperglycemic and T2D animal models, GK rat and db/db mouse islets³⁴ as well as by environmental stress in the form of high glucose and palmitate in human islets, Wistar rat islets, and clonal cells (Fig. 1). Interestingly, $Ca_v\gamma 4$ expression is unaffected in Akita mouse islets, a model of ER stress, may suggests that $Ca_v\gamma 4$ action occurs earlier in glucotoxicity. $Ca_v\gamma 4$ is involved in regulation of L-type Ca^{2+} channel gene expression, as demonstrated here in human islets for both $Ca_v1.2$ and $Ca_v1.3$ (Fig. 4b, c,

Supplementary Fig. 4a), as well as on protein levels in INS-1 cells (Fig. 4d). Accordingly, $Ca_v\gamma 4$ correlated evidently with $Ca_v1.2$ and $Ca_v1.3$ in human islets microarray analysis (Fig. 4a), and exhibited a direct interaction with $Ca_v1.3$ in INS-1 cells (Fig. 4g, h). By contrast, the impact of $Ca_v\gamma 4$ on expression of the other L-type channels, the predominantly skeletal $Ca_v1.1$ and retinal $Ca_v1.4$ (ref. 3), were very weak (Fig. 4a). Interestingly, $Ca_v\gamma 4$ is expressed throughout the entire cell volume in human beta cells (Fig. 1b), which differs from previous observations by electron microscopy that $Ca_v\gamma 4$ locates close to the plasma membrane³⁵. The demonstrated direct interaction between $Ca_v\gamma 4$ and $Ca_v1.3$ (Fig. 4g, h) suggests effects on modulating Ca^{2+} influx by, e.g., facilitating L-type Ca^{2+} channel trafficking, internalization, and degradation, but also potential functions completely unrelated to



Ca²⁺ homeostasis, which will be explored in future. Be that as it may, Ca $v\gamma 4$ clearly determines beta-cell functionality by enhancing Ca²⁺ entry through L-type Ca²⁺ channels. The specificity of Ca $v\gamma 4$ for modulating L-type Ca²⁺ currents is demonstrated by the fact that L-type Ca²⁺ channel blocker isradipine was

ineffective in Ca $v\gamma 4$ -silenced cells. In agreement with this finding, Ca $v\gamma 4$ did not influence the amplitude of non-L-type Ca²⁺ currents (Fig. 3l). Interestingly, the reduced Ca²⁺ influx and exocytosis in T2D human and GK rat beta cells were rescued when overexpressing Ca $v\gamma 4$ (Figs. 3b, d and 2g, h), and insulin

Fig. 5 $Ca_v\gamma 4$ is downregulated by silencing of the transcription factor MafA. **a** Rank of Pearson correlation coefficient (R) (tested by t -test) calculated by mRNA expression (Microarray, human islets) between $Ca_v\gamma 4$ (*CACNG4*) and the transcription factors known for pancreas development. $n = 128$ donors. **b** $Ca_v\gamma 4$ mRNA expression in *Pdx1*, *NeuroD1*, *MafA*, *Isl1*, or *Tcf7l2* silenced INS-1 cells. $n = 3$, $**p = 0.001$ (*NeuroD1*), $***p < 0.001$ (*MafA*), $*p = 0.016$ (*Isl1*). **c** As in **b** but $Ca_v\gamma 4$ protein expressions were measured. $n = 3$, $***p < 0.001$ (*Pdx1*, *NeuroD1*, *MafA*, *Isl1*), $**p = 0.007$ (*Tcf7l2*). **d** Decreased $Ca_v\gamma 4$ expression in *MafA* ^{$\Delta\beta$ cell} islets. $n = 3$ mice each, $**p = 0.001$. **e** $Ca_v\gamma 4$ mRNA expression was reduced in *MAFA* and *MAFB* double-silenced human islets. $n = 5$ donors, $**p = 0.005$. **f** qPCR amplification of $Ca_v\gamma 4$ (*Cacng4*) regulatory sequences after immunoprecipitation of chromatin transfected with myc-tagged MafA in β TC6 cells. Data are presented as %input. $n = 4$ (−63 bp) and 6 (+1683 bp), respectively, $**p < 0.01$. **g** *ALDH1A3* mRNA expression in $Ca_v\gamma 4$ -overexpressed human islets. $n = 3$ donors, $**p = 0.004$. **h** *Aldh1a3* protein expression in $Ca_v\gamma 4$ -silenced INS-1 cells (96 h). $n = 4$, $**p = 0.008$. Data are presented as mean \pm SEM and were analyzed with two-tailed unpaired Student's t -test, and the significance in **b**, **c** was corrected by the Holm-Bonferroni method. WT wild type, Ctrl control, KD knockdown

secretion was also partly recovered in T2D human and GK rat islets (Fig. 2b, d). In summary, $Ca_v\gamma 4$ plays a more important role than anticipated for Ca^{2+} signaling in beta cells and appears to be a central player in the regulation of insulin secretion (Fig. 2 and Supplementary Fig. 2). For future studies, the molecular structural mechanisms by which $Ca_v\gamma 4$ connects to the L-type $\alpha 1$ subunits will be an important issue to resolve.

Ca_v channels have dual roles and are key for regulation of gene expression and beta-cell differentiation^{4,36,37}. They generate Ca^{2+} signals that activates specific Ca^{2+} -dependent pathways that control gene expression^{36–39}. During the process of differentiation, transcription factors regulate Ca_v channel subunits expression. This generates a controlled temporal pattern of activating Ca^{2+} signals for the above-mentioned transcriptional effects⁴⁰. In beta cells, the transcription factor MafA is responsible for beta-cell-specific expression of insulin and also reprograms adult pancreatic acinar cells into beta-like cells by incompletely elucidated mechanisms²⁰. Importantly, the nuclear levels of MafA are drastically and specifically reduced in oxidative stressed beta cell lines, *db/db* mouse, and T2D human islets, whereas *Pdx1*, *Isl1*, and *NeuroD1* are unaffected under such conditions⁴¹.

Ca^{2+} transients in the cytosol have been implicated in initiating differentiation of mesenchymal cells⁴². These transients originate either from intracellular stores or from influx of extracellular Ca^{2+} through Ca_v channels in response to membrane depolarization. $Ca_v\gamma 4$ is highly expressed in the fetal brain, as well as in the subpopulation of differentiating myoblasts and has been suggested to play an important role in regulating intracellular Ca^{2+} transients¹⁸. The present study shows that in human islets $Ca_v\gamma 4$ is correlated with many transcription factors known in pancreas development or endocrine cell differentiation (Fig. 5a). Notably, we here provide evidence for $Ca_v\gamma 4$ being one of the downstream targets of MafA and one that has profound impact on the mature beta-cell phenotype. First, MafA exhibits a strong positive correlation to $Ca_v\gamma 4$ in human islets (Supplementary Fig. 5a). Second, expression of $Ca_v\gamma 4$ is markedly reduced in *MafA* ^{$\Delta\beta$ cell} islets, *MAFA* and *MAFB* double-depleted human islets, as well as MafA silenced INS-1 cells, with equally strong alteration of voltage-gated L-type Ca^{2+} currents, and in turn, $[Ca^{2+}]_i$, exocytosis and insulin release (Figs. 5 and 6). Most importantly, MafA directly binds to the promoter region of $Ca_v\gamma 4$ (Fig. 5f). In addition, the fact that MafA levels are markedly reduced in beta cells upon chronic oxidative stress as glucose toxicity develops is well established^{41,43,44}. Collectively, these results demonstrate the connection between glucotoxicity, differentiation, gene expression, and functional consequences (Ca^{2+} signaling, secretion) for the beta-cell. In the human microarray data set, $Ca_v\gamma 4$ exhibited the strongest correlation with *MAFB* among all transcription factors (Fig. 5a). Given that in rodents MafB is exclusively expressed in adult alpha-cell, whereas MafA is necessary for adult beta-cell function, we hence focused on the effect of MafA on $Ca_v\gamma 4$ in the present study. However, MafB is crucial for both alpha- and beta-cell

differentiation during islet development and has also been detected in adult human beta cells^{20,26,29}, a future thorough investigation of the interactions between MafB and $Ca_v\gamma 4$ is warranted. Besides MafA, in another high-throughput CHIP-on-chip data set of global *Pdx1* occupancy revealed that *Pdx1* also directly binds to the promoter region of *Cacng4* ($Ca_v\gamma 4$) in mouse Min6 cells⁴⁵. Moreover, MafA was strongly downregulated in both acute *Pdx1*-deficient Min6 cells and chronic *Pdx1* heterozygous (*Pdx1*^{+/-}) mouse islets⁴⁵. This taken together with our data to the effect that silencing of MafA (and/or *Pdx1*) results in reduced $Ca_v\gamma 4$ protein levels (Fig. 5c), strongly suggests that $Ca_v\gamma 4$ is a direct target of MafA (and *Pdx1*) in regulating beta-cell differentiation. Interestingly, $Ca_v\gamma 4$ expression was also regulated by *NeuroD1*, *Isl1*, and *Tcf7l2* in the current study (Fig. 5b, c). Here we hypothesize that the transcription factors interact with the promoter of $Ca_v\gamma 4$ gene by a direct binding (*NeuroD1*, *Isl1*) or an indirect impact through MafA or *Tcf7l2* (ref. 25). To identify the underlying mechanisms, future studies are warranted on how $Ca_v\gamma 4$ and other Ca_v channels are transcribed, translated, and transported to plasma membrane.

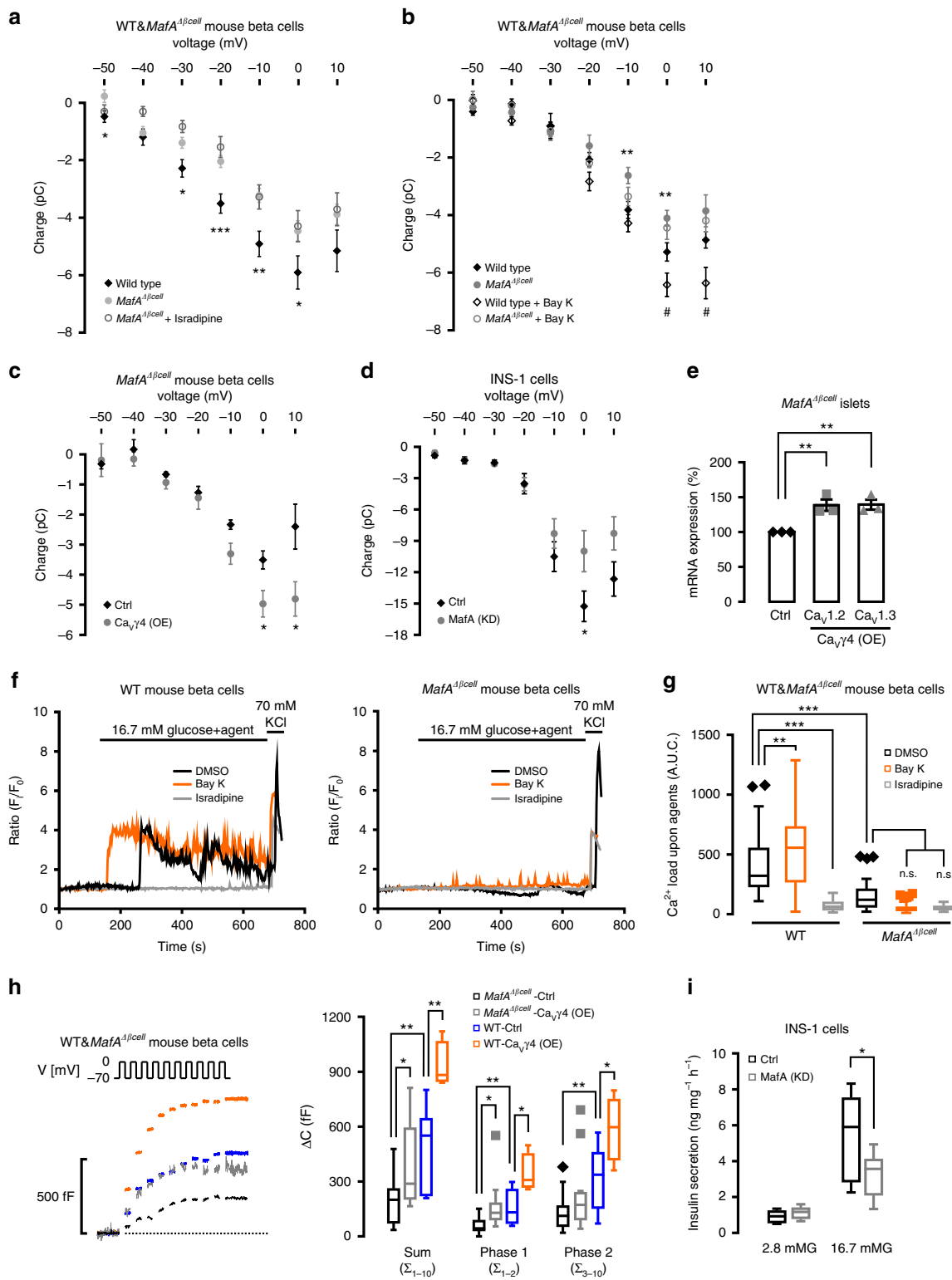
Aldh1a3 has long been recognized as a standard marker of cancer precursor cells⁴⁶, but was recently reported to be elevated in beta-cell dedifferentiated animal model, and it is now regarded an endocrine progenitor cell marker^{22,30}. This agrees with data in the current study to the effect that alteration of $Ca_v\gamma 4$ expression leads to changes in *Aldh1a3* expression in both human islets and INS-1 cells (Fig. 5g, h, Supplementary Fig. 5c), while not affecting cell viability, apoptosis, or proliferation (Supplementary Fig. 5d–f).

In conclusion, we demonstrate an essential role of the $Ca_v\gamma 4$ subunit for maintaining the normal pancreatic beta-cell phenotype in humans. This resonates well with the emerging view that Ca_v channels exert long-term effects on gene expression and RNA editing^{11,37}. $Ca_v\gamma 4$ is part of the MafA pathway that controls the final stage of beta-cell differentiation, and is suppressed in vivo and in vitro by hyperglycemic stress. Taken together, these results indicate a fundamental role for Ca_v -generated signals in long-term regulation of the beta-cell functional status in health and disease.

Methods

Human islets. Human pancreatic islets were obtained provided through collaboration between Human Tissue Laboratory within Lund University and the Nordic Network for Clinical Islet Transplantation (Uppsala University, Sweden). The human islets (70–90 % purity) had been cultured in CMRL 1066 (ICN Biomedicals, Costa Mesa, CA) supplemented with 10 mM HEPES, 2 mM L-glutamine, 50 μ g ml⁻¹ gentamicin, 0.25 μ g ml⁻¹ fungizone (Gibco, BRL, Gaithersburg, MD), 20 μ g ml⁻¹ ciprofloxacin (Bayer Healthcare, Leverkusen, Germany), and 10 mM nicotinamide at 37 °C (5% CO₂) for 1–5 days prior to the arrival in the laboratory. The islets were then handpicked under a stereomicroscope. All procedures were approved by the ethics committees at Uppsala and Lund Universities. See Supplementary Table 1 for the characteristics of human islet donors.

Animals. Adult beta-cell MafA deletion mutant mice were generated using the *Cre-loxP*-mediated recombination system. The *MafA*^{*fl/fl*}, *MafA*^{-/-}, and *RIP* (*rat*



insulin promoter-*cre* mouse lines have been generated previously⁴⁷. The *RIP-Cre* mouse line does not contain the human growth hormone minigene, which is in contrast to other commonly used pancreas-specific Cre deleter lines, which exhibit defects associated with the ectopic expression of human growth hormone in islets. In brief, a conditional *MafA* allele was generated earlier, and a *MafA* deletion in adult beta cells was achieved by crossing *MafA*^{Δβcell} mice with mice expressing Cre Recombinase under the rat insulin promoter (*RIP-cre*). *RIP-cre* mice were referred to as *MafA*^{Δβcell} mutants and resulted in complete loss of *MafA* expression,

impaired glucose clearance after an intraperitoneal glucose challenge⁴⁷. Mice were maintained on a mixed C57BL/6 and Sv129 background.

Wistar and GK male rats (Charles River Laboratories, Wilmington, MA) 6–11 week of age was used. Blood glucose at termination was measured to ensure the normoglycemic level for Wistar and hyperglycemia for GK. Adult *db/db* and control (C57/bl) mice (Janvier Laboratory, France), and Akita (*Ins2*^{+/-}) and wild-type (*Ins2*^{+/+}) male littermates (Jackson laboratories, stock number 003548) were used (7–13 weeks) for the indicated experiment. All animal experimentation was

Fig. 6 Reduced Ca^{2+} currents and GSIS by silencing of MafA. **a** Whole-cell Ca^{2+} charge-voltage relations in beta cells from wild-type mice, *MafA $\Delta\beta\text{cell}$* and *MafA $\Delta\beta\text{cell}$* in the presence of 2 μM isradipine. $n = 13, 15,$ and 7 cells, respectively, $p = 0.024^*, 0.020^*, 0.004^{**}, 0.036^*$ and $p < 0.001^{***}$ for $-50, -30, -10, 0,$ and -20 mV, respectively. **b** As in **a** but in wild type and *MafA $\Delta\beta\text{cell}$* beta cells in the absence ($n = 17$ wild type and 16 mutant cells) or presence ($n = 19$ wild type and 21 mutant cells) of 300 nM Bay K8644. $^{**}p = 0.006$ (-10 mV), $^{**}p = 0.008$ (0 mV) for wild type vs. *MafA $\Delta\beta\text{cell}$* ; $^{\#}p = 0.036$ (0 mV), $^{\#}p = 0.021$ (10 mV) for wild type in the absence or presence of Bay K8644. **c** As in **a** but in $\text{Ca}_v\gamma 4$ -overexpressed *MafA $\Delta\beta\text{cell}$* beta cells. $n = 5$ control and 8 overexpressing cells, $^*p = 0.035$ (0 mV), $^*p = 0.026$ (10 mV). **d** As in **a** but in MafA silenced INS-1 cells. $n = 15$ control and 18 silencing cells, $^*p = 0.046$. **e** $\text{Ca}_v1.2$ and $\text{Ca}_v1.3$ mRNA expression in $\text{Ca}_v\gamma 4$ overexpressed *MafA $\Delta\beta\text{cell}$* islets. $n = 3,$ $^{**}p = 0.009$ ($\text{Ca}_v1.2$), $^{**}p = 0.005$ ($\text{Ca}_v1.3$). **f** Intracellular Ca^{2+} concentration ($[\text{Ca}^{2+}]_i$) measured in wild type (left) and *MafA $\Delta\beta\text{cell}$* (right) beta cells by stimulation of 16.7 mM glucose in the presence of DMSO, Bay K8644 (300 nM), or isradipine (2 μM) for 600 s. **g** Ca^{2+} load in **f**, 0–600 s after stimulation. $n = 52$ (wild-type-DMSO), 65 (wild-type-BayK), 45 (wild-type-isradipine), 50 (*MafA $\Delta\beta\text{cell}$* -DMSO), 52 (*MafA $\Delta\beta\text{cell}$* -BayK), and 34 (*MafA $\Delta\beta\text{cell}$* -isradipine) cells; $^{**}p < 0.01,$ $^{***}p < 0.001,$ n.s. not significant. **h** Increased exocytosis in $\text{Ca}_v\gamma 4$ -overexpressed *MafA $\Delta\beta\text{cell}$* beta cells measured as ΔC (left), and the summary of data (right). $n = 13$ (*MafA $\Delta\beta\text{cell}$* -Ctrl), 13 (*MafA $\Delta\beta\text{cell}$* - $\text{Ca}_v\gamma 4$ (OE)), 8 (wild-type-Ctrl), and 4 (wild-type- $\text{Ca}_v\gamma 4$ (OE)) cells, $^*p < 0.05,$ $^{**}p < 0.01$. **i** Reduced GSIS (16.7 mM) in MafA silenced INS-1 cells. $n = 9,$ $^*p = 0.021$. Data are presented as mean \pm SEM and were analyzed with two-tailed unpaired Student's *t*-test (**a–e, h, i**) and one-way ANOVA with Tukey's multiple comparisons test (**g**); and the significance in **h** was corrected by the Holm-Bonferroni method. WT wild type, Ctrl control, KD knockdown, OE overexpression

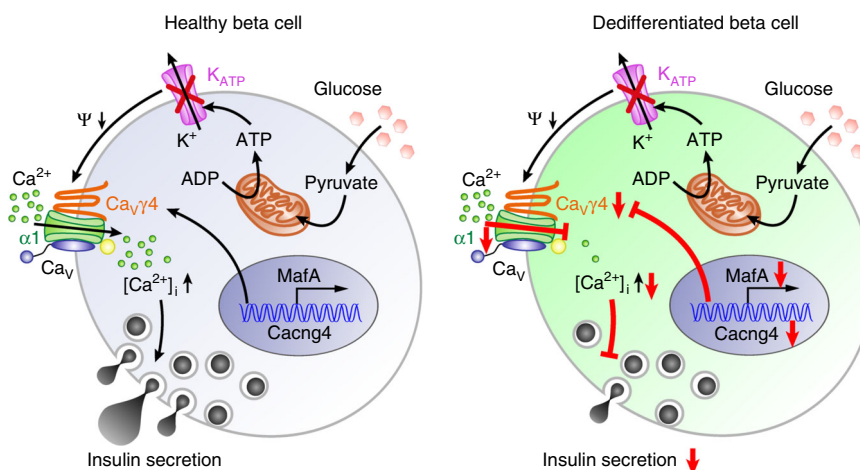


Fig. 7 Schematic of regulation cascade from MafA through $\text{Ca}_v\gamma 4$ to insulin secretion in beta cell. Compared with healthy beta cell, dedifferentiated beta cell caused by T2D or glucotoxicity results in reduced MafA expression, which leads to the downregulation of its direct downstream target $\text{Ca}_v\gamma 4$. Decreased $\text{Ca}_v\gamma 4$ expression then diminishes L-type Ca_v channels expression with consequent preventing of Ca^{2+} influx and in turn blunting of GSIS

conducted in accord with accepted standards of humane animal care and approved by the local ethics committee.

Human pancreatic islets microarray data. Human islets whole transcript microarray analysis was performed using GeneChip Human Gene 1.0 ST and processed with the standard Affymetrix protocol. The array data were then summarized and normalized with the Robust Multi-array Analysis (RMA) method using the oligo package from BioConductor. Batch correction was done with COMBAT function from SVA package from BioConductor. Annotation was done using annotate package from BioConductor and hugene10sttranscriptcluster.db annotation data. Probesets were only kept if they matched uniquely to a gene in the latest hg19 human genome assembly. If more than one probeset matched a gene, one probeset at random was chosen in order to have only one probeset per gene. Finally, only probesets (or genes) mapped to the autosomes were kept²⁴.

Cell culture. INS-1 832/13 cells (kindly donated by Dr. C. B. Newgaard, Duke University, USA) were cultured in RPMI-1640 containing 11.1 mM D-glucose and supplemented with 10% fetal bovine serum, 100 U ml⁻¹ penicillin (Gibco), 100 μg ml⁻¹ streptomycin (Gibco), 10 mM N-2 hydroxyethylpiperazine-N'-2-ethanesulfonic acid (HEPES), 2 mM glutamine, 1 mM sodium pyruvate, and 50 μM β -mercaptoethanol (Sigma), at 37 °C in a humidified atmosphere containing 95% air and 5% CO₂.

EndoC- β H1 cells (EndoCells, Paris, France) were maintained in a culture medium containing: DMEM (5.6 mM glucose), 2% BSA fraction V (Roche), 10 mM nicotinamide (Merck), 50 μM 2-mercaptoethanol, 5.5 μg ml⁻¹ transferrin, 6.7 ng ml⁻¹ sodium selenite (Sigma), 100 U ml⁻¹ penicillin, and 100 μg ml⁻¹ streptomycin (PAA Laboratories). For β -TC6 cell culture see below.

Islets isolation and preparation. Intact primary pancreatic islets were isolated by retrograde injection of a collagenase solution via the pancreatic duct from fed rats and 2-month old wild type and mutant mice, and were handpicked under a stereomicroscope at room temperature. The isolated islets were kept in RPMI-1640 medium for culture, but substituted with 5 mM D-glucose (for rats) or 10 mM D-glucose (for mice) and lack of β -mercaptoethanol. All indicated experiments were conducted on freshly isolated islets.

To perform electrophysiology and Ca^{2+} imaging experiments, the isolated islets were dispersed into single cells using Ca^{2+} -free buffer and allowed to adhere in 35-mm Petri dishes (Nunc, Thermo Scientific) coated by poly-L-lysine (Sigma) and cultured as above.

siRNA transfection. INS-1 832/13 cells were seeded 1 day before transfection. Thirty nanomolar RNA interference oligonucleotides (Ambion, USA) or Negative Control #1 (Ambion, USA) were applied to silence target genes. Transfection reagent (Dharmafect, Thermo Scientific, USA) was used. For primary human and rat islets, reverse transfection was performed to reach a faster and high-throughput transfection. Islets and siRNA-lipid complexes were prepared on the same day with Lipofectamine RNAiMAX (Invitrogen, USA) as transfection reagent. Transfection efficiency was measured by real-time PCR, western blotting, and visualized by BLOCK-iT Alexa Fluor Red Fluorescent Control (Invitrogen, USA).

Lentiviral transfection. Cacng4 or control (lentiviral particles without targeting any specific region) plasmids cloned in Lentiviral based shuttle vectors with mGFP tagged (ORIGENE, USA) were transformed into *E. coli* on LB-agar plates supplemented with 34 μg ml⁻¹ chloramphenicol. Amplified plasmids were purified with QIAGEN Plasmid Midi Kit (QIAGEN, USA). Lentiviral vectors were produced through transfection into HEK293T cells, and harvested followed by concentration and titration by service from Lund University Stem Cell Center Vector

Unit. Primary Human, rat or mouse islets and EndoC cells were transfected with *Cacng4* or control lentiviral vectors by directly adding into the culture medium under the calculation of 1 multiplicity of infection (MOI) for 72 h (change with fresh medium after 48 h transfection, and incubate another 24 h), followed by specific experiments indicated in results. Successful transfection was validated by qPCR, western blotting, and visualized through UV light under microscopy.

Insulin secretion. Transfected INS-1 832/13 cells were firstly washed twice with 1 ml pre-warmed Secretion Assay Buffer (SAB), pH 7.3 (114 mM NaCl, 4.7 mM KCl, 1.2 mM KH_2PO_4 , 1.16 mM MgSO_4 , 20 mM HEPES, 2.5 mM CaCl_2 , 25.5 mM NaHCO_3 , and 0.2% bovine serum albumin) supplemented with 2.8 mM glucose. The cells were then preincubated for 2 h in 1 ml new SAB with 2.8 mM glucose at 37 °C. Afterwards, insulin secretion was induced by static incubation with either 2.8 or 16.7 mM glucose for 1 h in 0.5 ml SAB, respectively. Secreted insulin was measured through the insulin Coat-a-Count RIA (Siemens Healthcare Diagnostics, IL, USA) by running on the 2470 WIZARD2 Automatic Gamma Counter (PerkinElmer, USA) or through high range rat insulin ELISA kit (Mercodia, Sweden), and normalized according to total protein content per well. Protein content was determined by Pierce BCA protein assay kit (Thermo Scientific, USA).

Transfected primary human or rat islets were preincubated with Krebs Ringer bicarbonate buffer (KRB), pH 7.4 (120 mM NaCl, 4.7 mM KCl, 2.5 mM CaCl_2 , 1.2 mM KH_2PO_4 , 1.2 mM MgSO_4 , 25 mM NaHCO_3 , 10 mM HEPES, and 1 mg ml⁻¹ BSA) for 30 min containing 2.8 mM glucose at 37 °C. Each incubation vial contained 12 size-matched islets in 1 ml KRB buffer and was treated with 95% O_2 and 5% CO_2 to obtain constant pH and oxygenation. After preincubation, the buffer was changed to 1 ml KRB buffer supplemented with either 2.8 or 16.7 mM glucose. The islets were then incubated for 1 h at 37 °C in a metabolic shaker (30 cycles per min). Immediately after incubation an aliquot of the medium was removed for analysis of secreted insulin and the islets were homogenized for measurement of insulin content using rat insulin RIA kit (Merck Millipore, Germany) or human insulin ELISA kit (Mercodia, Sweden). For each individual, measurements were performed in 6–8 vials per condition.

Electrophysiology. Whole-cell capacitance and whole-cell Ca^{2+} current measurements were performed in INS-1 832/13 cells or primary human, rat or mouse beta cells using HEKA EPC10 patch-clamp amplifiers with the software suite Pulse + X-Chart Extension (version 8.6 or later; HEKA, Lambrecht-Pfalz, Germany)⁴⁸. Primary islet cells or INS-1 832/13 cells were seeded in Nunc plastic Petri dishes and were used for experiments the following day. The bath was continuously perfused with extracellular solution containing 118 mM NaCl, 20 mM tetraethylammonium chloride, 5.6 mM KCl, 2.6 mM CaCl_2 , 1.2 mM MgCl_2 , 5 mM HEPES, and 5 mM glucose (pH 7.4 with NaOH), and the temperature maintained at 32 °C. The pipette (intracellular) solution consisted of 125 mM Cs-glutamate, 10 mM CsCl, 10 mM NaCl, 1 mM MgCl_2 , 5 mM HEPES, 3 mM Mg-ATP, 0.1 mM cAMP, and 0.05 mM EGTA (pH 7.2 with CsOH). 0.05 mM EGTA was replaced by 1.5 mM Bapta in the pipette solution for Ca^{2+} currents recording. L-type Ca^{2+} channel blocker isradipine (2 μM , Sigma), potentiation Bay K8644 (300 nM, Sigma), P/Q-type channel blocker ω -agatoxin IVA (100 nM, Alomone labs), N-type channel blocker ω -conotoxin GVIA (50 nM, Alomone labs), and R-type channel blocker SNX-482 (100 nM, Alomone labs) were added as indicated in text or figures. The whole-cell configuration was used in voltage-clamp mode and pipettes had an average resistance of \approx 5.5 M Ω . Beta- and alpha-cells were identified by the virtue of Na^+ channel inactivation features, with beta cells exhibiting half-maximal Na^+ channel inactivation at membrane potentials lower than -100mV and alpha-cells greater than -100mV ⁴.

Quantitative PCR. Total RNA was extracted using the RNeasy Kit (QIAGEN, Germany) after transfection. One microgram of RNA was used for cDNA synthesis. Primers of housekeeping genes *HPRT1*, *B2M*, and *POLR2A* (TaqMan Gene Expression, USA) and genes of interest (TaqMan Gene Expression) which tagged FAM dyes were used for amplification detection. The real-time PCR was carried out as follows: 50 °C for 2 min, 95 °C for 10 min, 40 cycles of 95 °C for 15 s, and 60 °C for 1 min by running on a ViiA 7 Real-Time System (Applied Biosystems) with total reaction mixture (10 μl) consisting of 5 μl TaqMan Universal PCR Master Mix (Applied Biosystems), 2.5 μl 4 \times primer, and cDNA.

Western blotting. INS-1 832/13 cells or primary islets were homogenized in ice cold RIPA buffer containing complete protease inhibitor (Roche) by vortex or shaking on ice for 30 min. Supernatant was collected by centrifugation (10,000 \times g, 15 min, 4 °C). Extracted total protein content was measured by Pierce BCA Protein Assay Kit (Thermo Scientific), and 10–20 μg of protein was electrophoresed on 4–15% SDS-PAGE (BIO-RAD). The separated proteins were then transferred onto a PVDF membrane (BIO-RAD), followed by blocking with 5.0% nonfat dry milk in TBST (Tris-buffered saline with Tween 20) (pH 7.4; 0.15 M NaCl, 10 mM Tris-HCl, and 0.1% Tween 20) for 1 h at room temperature. Afterwards, the membrane was incubated overnight at 4 °C with anti-*Ca_vγ4* (1:400; Alomone labs), *Ca_v1.2* (1:500; Sigma), *Ca_v1.3* (1:400; Abcam), *Ca_vα2δ1* (1:500; Abcam), *Ca_vβ1* (1:500; Abcam), *Aldh1a3* (1:1000; Abcam), *Cleaved Caspase-3* (1:1000; Cell Signaling), *P21* (1:1000; Abcam) antibodies followed by incubation with anti-rabbit IgG

(1:2000; Cell Signaling) or goat anti-mouse IgG (1:2000; Dako) at least 1 h at room temperature. Normalization was carried out by incubating membrane with anti-β actin (1:2000; Sigma) or PPIB (1:2000; Abcam) antibodies, or by the corresponding total protein. Immunoreactivity was detected using an enhanced chemiluminescence reaction (Pierce, Rockford, IL, USA) by SuperSignal West Femto Maximum Sensitivity Substrate (Thermo Scientific).

Immunostaining and confocal imaging. Isolated human islet cells were seeded on glass-bottomed dishes and cultured overnight. Then the cells were fixed by 3% PFA for 30 min and permeabilized with Perm Buffer III (BD, USA) for 30 min. The primary antibodies of rabbit anti-*Ca_vγ4* (Abnova), Guinea pig anti-insulin (Eurodiagnostika) were diluted by 1:100 and 1:400, respectively, and incubated with cells overnight at 4 °C. Immunoreactivity was quantified using fluorescently labeled secondary antibodies: Alexa Fluor 647, Donkey anti-rabbit, red (1:300, Jackson ImmunoResearch), Cy 2, Donkey anti-guinea pig, green (1:300, Jackson ImmunoResearch). The Confocal images were acquired using a Zeiss 510 Meta LSM and a \times 63 oil immersion objective and the fluorescent intensity was analyzed with software ZEM 2009.

Chromatin immunoprecipitation. β-TC6 cells were maintained in Dulbecco's modified Eagle's medium (DMEM; Invitrogen) supplemented with 10% fetal bovine serum (FBS; Sigma) and 1% penicillin/streptomycin (PEST; Invitrogen). β-TC6 cells were transfected with myc-tagged MAFA and chromatin was prepared 3 days after transfection. Protein/DNA chromatin fragments were immunoprecipitated with rabbit anti-myc antibody (Novus) or mouse IgG (Jackson ImmunoResearch) as previously described⁴⁹. Enrichment was assessed by qPCR (StepOne, Life Technologies) and is presented as percent input. Primer sequences were +1683 bp forward TTTGTGAGGCGTCTTCC, +1683 bp reverse TGTCCTCCAATTCGGAGTCC, –63 bp forward TACAGCCAGTAGTCGGTGC, –63 bp reverse CTATGAGGCGCCACCAT. Albumin control promoter sequences were not detected in IgG and myc-immunoprecipitated DNA.

Ca^{2+} imaging. Twenty-four hours prior to Ca^{2+} imaging, the cells were transfected to glass-bottom dishes while diluted 1:6 (\sim 1 \times 10⁵ cells). Fluo-5F (Kd = 2.3 μM) (Invitrogen) was used for measuring intracellular Ca^{2+} concentration [Ca^{2+}]_i. The cells were loaded at room temperature for 30 min with Fluo-5F (1 μM) dissolved in the perfusion buffer (KRB) supplemented with 5 mM glucose. Stimulation was carried out by 16.7 mM glucose KRB buffer in the absence or presence of DMSO (1:1000) or Bay K8644 (300 nM) or isradipine (2 μM), and/or 70 mM KCl KRB buffer at room temperature. Time lapse region of interest (ROI) images, the mean and peak intensity of ROIs were acquired by confocal microscopy using a \times 40 water immersion objective. A ratio was calculated by taking the fluorescence intensity in the time lapse divided by the average fluorescence intensity under pre-stimulatory conditions. The frequency of peak intensity was counted as ratio >1.5, and the time integral of the fluorescence signal (AUC) was calculated by GraphPad software.

Duolink in situ detection. INS-1 832/13 cells were transferred on the μ -8-well plate (iBidi) 12–24 h before staining experiments. The cells were fixed by 3% PFA for 30 min and permeabilized with Perm Buffer III (BD, USA) for 40 min. The primary antibodies of rabbit anti-*Ca_vγ4* (Alomone labs) and mouse anti-*Ca_v1.3* (Abcam) were diluted by 1:100 and 1:200, respectively, and incubated with cells for overnight. The staining protocol followed instructions provided by the manufacturer and the spots were imaged by confocal microscopy and the spots numbers per cell were calculated by Duolink Image Tool (Olink Bioscience, Sweden).

Measurement of cellular viability (MTT) and apoptosis. The viability of cells was investigated in INS-1 cells silenced with *Ca_vγ4* siRNA for 72 h. Measurement was performed using the MTT reagent kit according to the manufacturer's instructions (Roche). To measure the cell apoptosis in living cells, 7-AAD (BD Pharmingen) staining was used in 72 h *Ca_vγ4*-silenced INS-1 cells, and the positive cells were counted by confocal microscopy to indicate apoptotic cells.

Statistics. The data are presented as means \pm SEM for the indicated number of observations or different experiments, or presented as box-plots with whiskers created using Tukey's method. The significance of random differences was analyzed by Student's *t*-test. Pearson correlation coefficient (*R*) was used and tested (*t*-test) for a measure of the linear correlation between expression of genes. Holm–Bonferroni correction was used to adjust the rejection criteria of each of the individual comparisons for multiple groups, and one-way ANOVA with Tukey's test was used for multiple comparisons. *p* < 0.05 was considered as significant. **p* < 0.05; ***p* < 0.01; ****p* < 0.001.

Reporting Summary. Further information on experimental design is available in the Nature Research Reporting Summary linked to this article.

Data availability

All human islet microarray data are MIAME compliant, and the raw data have been deposited in the Gene Expression Omnibus (GEO) database, www.ncbi.nlm.nih.gov/geo (accession no. GSE50398, GSE38642, and GSE44035). All source data underlying the graphs presented in the main figures are available as Supplementary Data. All other data generated and/or analyzed during the current study are available from the corresponding author on reasonable request.

Received: 2 August 2018 Accepted: 8 February 2019

Published online: 15 March 2019

References

- Porte, D. Jr. Banting lecture 1990. Beta-cells in type II diabetes mellitus. *Diabetes* **40**, 166–180 (1991).
- Rorsman, P. & Renstrom, E. Insulin granule dynamics in pancreatic beta cells. *Diabetologia* **46**, 1029–1045 (2003).
- Yang, S. N. & Berggren, P. O. The role of voltage-gated calcium channels in pancreatic beta-cell physiology and pathophysiology. *Endocr. Rev.* **27**, 621–676 (2006).
- Jing, X. et al. CaV2.3 calcium channels control second-phase insulin release. *J. Clin. Invest.* **115**, 146–154 (2005).
- Hoppa, M. B., Lana, B., Margas, W., Dolphin, A. C. & Ryan, T. A. alpha2delta expression sets presynaptic calcium channel abundance and release probability. *Nature* **486**, 122–125 (2012).
- Dolphin, A. C. Calcium channel diversity: multiple roles of calcium channel subunits. *Curr. Opin. Neurobiol.* **19**, 237–244 (2009).
- Black, J. L. 3rd The voltage-gated calcium channel gamma subunits: a review of the literature. *J. Bioenerg. Biomembr.* **35**, 649–660 (2003).
- Andronache, Z. et al. The auxiliary subunit gamma 1 of the skeletal muscle L-type Ca²⁺-channel is an endogenous Ca²⁺-antagonist. *Proc. Natl Acad. Sci. USA* **104**, 17885–17890 (2007).
- Yang, L., Katchman, A., Morrow, J. P., Doshi, D. & Marx, S. O. Cardiac L-type calcium channel (Cav1.2) associates with gamma subunits. *FASEB J.* **25**, 928–936 (2011).
- Wu, J. et al. Structure of the voltage-gated calcium channel Cav1.1 complex. *Science* **350**, aad2395 (2015).
- Du, X. et al. Second cistron in CACNA1A gene encodes a transcription factor mediating cerebellar development and SCA6. *Cell* **154**, 118–133 (2013).
- Reinbothe, T. M. et al. The human L-type calcium channel Cav1.3 regulates insulin release and polymorphisms in CACNA1D associate with type 2 diabetes. *Diabetologia* **56**, 340–349 (2013).
- Holmkvist, J. et al. Polymorphisms in the gene encoding the voltage-dependent Ca²⁺ channel Ca (V)_{2.3} (CACNA1E) are associated with type 2 diabetes and impaired insulin secretion. *Diabetologia* **50**, 2467–2475 (2007).
- Itariu, B. K. & Stulnig, T. M. Autoimmune aspects of type 2 diabetes mellitus—a mini-review. *Gerontology* **60**, 189–196 (2014).
- Talchai, C., Xuan, S., Lin, H. V., Sussel, L. & Accili, D. Pancreatic beta cell dedifferentiation as a mechanism of diabetic beta cell failure. *Cell* **150**, 1223–1234 (2012).
- Namkung, Y. et al. Requirement for the L-type Ca²⁺ channel alpha1D subunit in postnatal pancreatic beta cell generation. *J. Clin. Invest.* **108**, 1015–1022 (2001).
- Popiela, H. & Moore, W. Tolbutamide stimulates proliferation of pancreatic beta cells in culture. *Pancreas* **6**, 464–469 (1991).
- Kious, B. M., Baker, C. V., Bronner-Fraser, M. & Knecht, A. K. Identification and characterization of a calcium channel gamma subunit expressed in differentiating neurons and myoblasts. *Dev. Biol.* **243**, 249–259 (2002).
- Matsuoka, T. A. et al. The MafA transcription factor appears to be responsible for tissue-specific expression of insulin. *Proc. Natl Acad. Sci. USA* **101**, 2930–2933 (2004).
- Hang, Y. & Stein, R. MafA and MafB activity in pancreatic beta cells. *Trends Endocrinol. Metab.* **22**, 364–373 (2011).
- Santos, G. J. et al. Metabolic memory of ss-cells controls insulin secretion and is mediated by CaMKII. *Mol. Metab.* **3**, 484–489 (2014).
- Cinti, F. et al. Evidence of beta-cell dedifferentiation in human type 2 diabetes. *J. Clin. Endocrinol. Metab.* **101**, 1044–1054 (2016).
- Wang, Z., York, N. W., Nichols, C. G. & Remedi, M. S. Pancreatic beta cell dedifferentiation in diabetes and redifferentiation following insulin therapy. *Cell Metab.* **19**, 872–882 (2014).
- Fadista, J. et al. Global genomic and transcriptomic analysis of human pancreatic islets reveals novel genes influencing glucose metabolism. *Proc. Natl Acad. Sci. USA* **111**, 13924–13929 (2014).
- Zhou, Y. et al. TCF7L2 is a master regulator of insulin production and processing. *Hum. Mol. Genet.* **23**, 6419–6431 (2014).
- Artner, I. et al. MafA and MafB regulate genes critical to beta-cells in a unique temporal manner. *Diabetes* **59**, 2530–2539 (2010).
- Oliver-Krasinski, J. M. & Stoffers, D. A. On the origin of the beta cell. *Genes Dev.* **22**, 1998–2021 (2008).
- Wilson, M. E., Scheel, D. & German, M. S. Gene expression cascades in pancreatic development. *Mech. Dev.* **120**, 65–80 (2003).
- Dai, C. et al. Islet-enriched gene expression and glucose-induced insulin secretion in human and mouse islets. *Diabetologia* **55**, 707–718 (2012).
- Kim-Muller, J. Y. et al. Metabolic inflexibility impairs insulin secretion and results in MODY-like diabetes in triple FoxO-deficient mice. *Cell. Metab.* **20**, 593–602 (2014).
- Sharp, A. H. & Campbell, K. P. Characterization of the 1,4-dihydropyridine receptor using subunit-specific polyclonal antibodies. Evidence for a 32,000-Da subunit. *J. Biol. Chem.* **264**, 2816–2825 (1989).
- Chen, L. et al. Stargazin regulates synaptic targeting of AMPA receptors by two distinct mechanisms. *Nature* **408**, 936–943 (2000).
- Tomita, S. et al. Functional studies and distribution define a family of transmembrane AMPA receptor regulatory proteins. *J. Cell Biol.* **161**, 805–816 (2003).
- King, A. J. The use of animal models in diabetes research. *Br. J. Pharmacol.* **166**, 877–894 (2012).
- Sharp, A. H. et al. Biochemical and anatomical evidence for specialized voltage-dependent calcium channel gamma isoform expression in the epileptic and ataxic mouse, stargazer. *Neuroscience* **105**, 599–617 (2001).
- Shalizi, A. et al. A calcium-regulated MEF2 sumoylation switch controls postsynaptic differentiation. *Science* **311**, 1012–1017 (2006).
- Wheeler, D. G. et al. Ca(V)1 and Ca(V)2 channels engage distinct modes of Ca²⁺ signaling to control CREB-dependent gene expression. *Cell* **149**, 1112–1124 (2012).
- Naranjo, J. R. & Mellstrom, B. Ca²⁺-dependent transcriptional control of Ca²⁺+homeostasis. *J. Biol. Chem.* **287**, 31674–31680 (2012).
- Gomez-Ospina, N., Tsuruta, F., Barreto-Chang, O., Hu, L. & Dolmetsch, R. The C terminus of the L-type voltage-gated calcium channel Ca(v)1.2 encodes a transcription factor. *Cell* **127**, 591–606 (2006).
- Maki, T. et al. Regulation of calcium channel expression in neonatal myocytes by catecholamines. *J. Clin. Invest.* **97**, 656–663 (1996).
- Guo, S. et al. Inactivation of specific beta cell transcription factors in type 2 diabetes. *J. Clin. Invest.* **123**, 3305–3316 (2013).
- Lin, S. S. et al. Cav3.2 T-type calcium channel is required for the NFAT-dependent Sox9 expression in tracheal cartilage. *Proc. Natl Acad. Sci. USA* **111**, E1990–E1998 (2014).
- Robertson, R. P. Chronic oxidative stress as a central mechanism for glucose toxicity in pancreatic islet beta cells in diabetes. *J. Biol. Chem.* **279**, 42351–42354 (2004).
- Harmon, J. S., Stein, R. & Robertson, R. P. Oxidative stress-mediated, post-translational loss of MafA protein as a contributing mechanism to loss of insulin gene expression in glucotoxic beta cells. *J. Biol. Chem.* **280**, 11107–11113 (2005).
- Sachdeva, M. M. et al. Pdx1 (MODY4) regulates pancreatic beta cell susceptibility to ER stress. *Proc. Natl Acad. Sci. USA* **106**, 19090–19095 (2009).
- Marcato, P., Dean, C. A., Giacomantonio, C. A. & Lee, P. W. Aldehyde dehydrogenase: its role as a cancer stem cell marker comes down to the specific isoform. *Cell Cycle* **10**, 1378–1384 (2011).
- Ganic, E. et al. MafA-controlled nicotinic receptor expression is essential for insulin secretion and is impaired in patients with type 2 diabetes. *Cell Rep.* **14**, 1991–2002 (2016).
- Buda, P. et al. Eukaryotic translation initiation factor 3 subunit E controls intracellular calcium homeostasis by regulation of ocav1.2 surface expression. *PLoS ONE* **8**, e64462 (2013).
- Mazur, M. A. et al. Microphthalmia transcription factor regulates pancreatic beta-cell function. *Diabetes* **62**, 2834–2842 (2013).

Acknowledgements

Authors thank B.-M. Nilsson and A.-M. Veljonskaja-Ramsay (Lund University Diabetes Center, Sweden) for expert technical assistance. We are grateful to Elvira Ganic for help with *MafA^{Δβcell}* mouse islets preparation. We thank M. Magnusson for mouse strain maintenance. We also appreciate the supports from the Swedish Research Council, Strategic Research Area Exodiab (Dnr 2009-1039), Swedish Foundation for Strategic Research (Dnr IRC 15-0067) and Swedish Research Council, Linnaeus grant (Dnr 349-2006-237). This work was supported by a grant from the Diabetes Wellness foundation (to E.R.). Salaries and infrastructure were supported by the Swedish Research Council (to E.R., I.A., L.E., and E.Z.), the Juvenile Diabetes Research Foundation (I.A.), Diabetesfonden (E.R., I.A., and L.E.), the Crafoord foundation (to E.Z.), and the European Foundation for the Study of Diabetes (to I.A.).

Author contributions

E.R. and E.Z. designed and supervised the study, conducted data analysis and finalized manuscript writing with feedback from all authors. C.L. performed experiments on human islets, isolated rodent islets and INS-1 cells, conducted data analysis, and drafted the manuscript. Y.Y., T.S., and M.B. performed experiments. L.E. revised manuscript. I.A. provided *MafA^{Δβcell}* mice, designed experiments, and conducted data analysis. E.Z. conducted experiments and data analysis.

Additional information

Supplementary information accompanies this paper at <https://doi.org/10.1038/s42003-019-0351-4>.

Competing interests: The authors declared no competing interests.

Reprints and permission information is available online at <http://npg.nature.com/reprintsandpermissions/>

Publisher's note: Springer Nature remains neutral with regard to jurisdictional claims in published maps and institutional affiliations.



Open Access This article is licensed under a Creative Commons Attribution 4.0 International License, which permits use, sharing, adaptation, distribution and reproduction in any medium or format, as long as you give appropriate credit to the original author(s) and the source, provide a link to the Creative Commons license, and indicate if changes were made. The images or other third party material in this article are included in the article's Creative Commons license, unless indicated otherwise in a credit line to the material. If material is not included in the article's Creative Commons license and your intended use is not permitted by statutory regulation or exceeds the permitted use, you will need to obtain permission directly from the copyright holder. To view a copy of this license, visit <http://creativecommons.org/licenses/by/4.0/>.

© The Author(s) 2019